Cux2 Activity Defines a Subpopulation of Perinatal Neurogenic Progenitors in the Hippocampus

Makiko Yamada, Jessica Clark, Christine McClelland, Emily Capaldo, Ayush Ray, and Angelo Iulianella*

ABSTRACT: The hippocampus arises from the medial region of the sub-ventricular (SVZ) within the telencephalon. It is one of two regions in the postnatal brain that harbors neural progenitors (NPs) capable of giving rise to new neurons. Neurogenesis in the hippocampus is restricted to the sub-granular zone (SGZ) of the dentate gyrus (DG) where it contributes to the generation of granule cell layer (gcl) neurons. It is thought that SGZ progenitors are heterogeneous, differing in their morphology, expression profiles, and developmental potential, however it is currently unknown whether they display differences in their developmental origins and cell fate-restriction in the DG. Here we demonstrate that Cux2 is a marker for SGZ progenitors and nascent granule cell neurons in the perinatal brain. Cux2 was expressed in the presumptive hippocampal forming region of the embryonic forebrain from E14.5 onwards. At fetal stages, Cux2 was expressed in early-forming Prox1$^+$ granule cell neurons as well as the SVZ of the DG germinal matrix. In the postnatal brain, Cux2 was expressed in several types of progenitors in the SGZ of the DG, including Nestin/Sox2 double-positive radial glia, Sox2$^+$ cells that lacked a radial glial process, DCX$^+$ neuroblasts, and Calretinin-expressing nascent neurons. Another domain characterized by a low level of Cux2 expression emerged in Calbindin$^+$ neurons of the developing DG blades. We used Cux2-Cre mice in genetic fate-mapping studies and showed almost exclusive labeling of Calbindin-positive gcl neurons, but not in any progenitor cell types or astroglia. This suggests that Cux2$^+$ progenitors directly differentiate into gcl neurons and do not self-renew. Interestingly, developmental profiling of cell fate revealed an outside-in formation of gcl neurons in the DG, likely reflecting the activity of Cux2 in the germinative matrices during DG formation and maturation. However, DG morphogenesis proceeded largely normally in hypomorphic *Cux2* mutants lacking Cux2 expression. Taken together we conclude that Cux2 expression reflects hippocampal neurogenesis and identifies non-self-renewing NPs in the SGZ. © 2014 The Authors Hippocampus Published by Wiley Periodicals, Inc.

KEY WORDS: Cux2; neural progenitors; hippocampus; dentate gyrus development; fate map

INTRODUCTION

The hippocampus is one of two principal regions of the mammalian brain in which new neurons are continually generated throughout life. Classic birth dating studies by Altman and coworkers revealed that the subventricular zone (SVZ) of the lateral ventricle and the dentate gyrus (DG) of the hippocampus display ongoing neurogenesis well into adult stages (Altman and Das, 1965, 1966; Altman, 1969; Altman and Bayer, 1990b). The importance of neurogenesis in normal brain function is illustrated in rodent models for neurodegenerative diseases and brain injury, which not only display profound neuronal loss, but are also characterized by the aberrant regulation of neurogenesis and recruitment of nascent neurons in the hippocampus and forebrain (Nakatomi et al., 2002; Lichtenwalner and Parent, 2006; Zhang et al., 2007; Burns et al., 2009; Yu et al., 2009; Kernie and Parent, 2010; Lazarov et al., 2010; Lopez-Toledano et al., 2010; Wang et al., 2011). Yet to be resolved is the potentially heterogeneous origin of neural progenitors (NPs) in the hippocampus and whether they exhibit different abilities to respond to disease or injury during the lifespan of the organism.

The DG of the hippocampus is derived from the ventricular zone of the medial region of the lateral ventricle in the developing cortex (Altman and Bayer, 1990b; Li and Pleasure, 2005). The future granule cell neurons arise at fetal stages from progenitor populations lining this region and migrate inward to generate a SVZ of proliferating granule cell layer (gcl) precursors. In the SVZ granule cell, precursors are found adjacent to the developing dentate knot, where they proliferate rapidly to produce a secondary germinative matrix. The upward migration of immature granule cells from the ventricular surface progressively contributes to the formation of the DG in the SVZ of the medial cortex. In this manner the gcl of the DG is generated with the outer layer of the blades forming first, while the continued proliferation of granule cell precursors in the developing dentate matrix contributes to the formation of the inner gcl. In rodents, within the

first few weeks of life the progenitor cells of the DG become restricted to a specialized layer called the subgranular zone (SGZ) at the inner surface bordering the gcl of the DG (Altman and Bayer, 1990a,b). Hippocampal neurogenesis then becomes restricted to the SGZ throughout the life of the organism (Altman and Bayer, 1990a,b; Sohur et al., 2006; Ming and Song, 2011).

Beginning with the division of a progenitor cell and ending with the integration of a functional neuron, neurogenesis in the postnatal hippocampus is thought to involve a series of transitory cell types. In the adult DG, a Type 1 NP is characterized by a pyramidal morphology possessing a radial process and the expression of Nestin, glial fibrillary acidic protein (GFAP), and Sox2 (Seri et al., 2004, 2001; Kempermann et al., 2004; Kempermann, 2006). These cells are thought to differentiate into rapidly dividing transit-amplifying (Type 2b) cells characterized by the expression of Tbr2 (Hodge et al., 2008). The amplifiers are thought to give rise to neuroblasts (Type 3 cells) characterized by the expression of Doublecortin (DCX) and polysialic acid-neural cell adhesion molecule (PSA-NCAM), and ultimately differentiate into gcl interneurons (Seki and Arai, 1999). Type I NPs are also capable of asymmetrical divisions, resulting in self-renewal and the generation of a non-radial progenitor, which exhibits reduced Nestin and continued Sox2 expression, referred to as a Type 2a cell, can also give rise to neuroblasts (D'Amour and Gage, 2003; Ferri et al., 2004; Bonaguidi et al., 2011). Type 2a cells are thought to transition to neuroblasts via the Type2b amplifier, which expresses the transcription factor Tbr2 (Hodge et al., 2008). But it has not been clearly established whether Type 1 cells are exclusively self-renewing multipotent NPs, or instead represent a heterogeneous population of precursors displaying a limited capacity for self-renewal and restricted cell fate potential (Bonaguidi et al., 2011; Clarke and van der Kooy, 2011; Encinas et al., 2011; Kempermann, 2011). This is due in part to our limited knowledge of the developmental biology of SGZ progenitor cells, which has not greatly advanced beyond the birth dating studies by Altman and Bayer (1990a,b). It has been shown that at least some of the progenitors that populate the SGZ of the postnatal hippocampus have their origin in the germinative fetal neuroepithelium lining the ventricular zone (Clarke and van der Kooy, 2011). In order to shed light on the heterogeneity of SGZ progenitors, we need to better define their developmental origins and their intrinsic regulators.

In this study, we evaluated the role of the Cut-like transcription factor Cux2 as a novel discriminatory marker for neurogenic progenitors in the developing and postnatal hippocampus. Our previous findings showed that Cux2 is required for neurogenesis in the developing spinal cord and olfactory epithelium (Iulianella et al., 2008; Wittmann et al., 2014), and others showed it regulates the formation of cortical pyramidal neurons from SVZ progenitors (Zimmer et al., 2004; Cubelos et al., 2008a; Franco et al., 2012). Cux2 fate-mapping studies in the cortex suggest that Cux2 activity biases the development of cortical SVZ precursors to layer II/II pyramidal neurons (Franco et al., 2012). However, a more recent study argues that Cux2^{+} progenitors can become both upper and deeper layer neurons in the developing cortex (Guo et al., 2013). It is therefore unclear whether Cux2 activity acts within NPs to restrict their development to particular neuronal fates and/or directs nascent neurons to particular laminar regions of the developing brain. It is also unknown whether Cux2 functions in the neurogenic regions of the postnatal brain, such as the hippocampus.

We investigated this possibility by characterizing the role of Cux2 in progenitor development in the SGZ of the perinatal hippocampus. We show that high levels of Cux2 expression were detected in the SGZ of the perinatal hippocampus. Cux2 co-localized with most identified types of SGZ progenitors, including the Type 1 Nestin[+]/Sox2^{+} cells, the Sox2^{+} Type 2a cells, as well as DCX[+] neuroblasts. EdU pulsing experiments revealed that Cux2 was expressed in non-dividing SGZ progenitors. Furthermore, we also observed a weaker level of expression in the outer granule cells of the maturing DG, suggesting Cux2 expression is under dynamic regulatory control in progenitors as they transition to mature granule cells. Interestingly, cell fate mapping using a Cux2-Cre transgenic mouse strain revealed restricted labeling of Calbindin^{+} DG cells in an outside-in manner, reminiscent of the expression of Cux2 during layer formation in neocortex. Altogether, this suggests that Cux2 may be a discriminatory maker for hippocampal progenitors that undergo directed differentiation into granule cells and do not self-renew.

MATERIALS AND METHODS

Animals

Cux2[neo/neo] hypomorphic mice were generated and genotyped as described (Iulianella et al., 2008). The *Cux2* mutant mice display highly reduced Cux2 protein levels in the brain and variable penetrance and expressivity of the phenotype (Iulianella et al., 2008). Although minor embryo lethality was reported, most *Cux2[neo/neo]* mutant mice were born viable and fertile and appeared grossly normal. We confirmed that *Cux2[neo/neo]* mutants lacked Cux2 expression in the postnatal hippocampus (Supporting Information Fig. S1). Experiments were performed on C57Bl/6 (The Jackson Laboratory, Bar Harbor, ME), *Cux2[neo/+]*, and *Cux2[neo/neo]* fetuses at embryonic (E) day 14.5–E18.5, and postnatal (P) day 10 to P21, and 3–8 months of age. This study was approved by the Dalhousie animal ethics committee and the animals were handled in accordance with the institutional regulations and guidelines of the Canadian Council on Animal Care.

Histology and Immunohistochemistry

Mice were anaesthetized and perfused with 0.9% saline and subsequently with ice-cold 4% paraformaldehyde (PFA)/0.1 M phosphate buffer (PB) or PBS. Brains were taken out, bisected along the midline, and fixed 6 h to overnight at 4°C. Tissues were equilibrated in sucrose, embedded in Optimum Cutting Temperature (OCT) compound (Tissue-Tek, Torrance, CA), and cryosectioned at 12–14 μm. Immunostaining was performed as described previously (Iulianella et al., 2008). The following antibodies were

used for immunohistochemistry: anti-Cux2 (1:1,000; Iulianella et al., 2008), anti-GFAP (GA5, 1:500; Millipore, Billerica, MA), anti-Sox2 (1:200; Santa Cruz Biotechnology, Santa Cruz, CA; 1:250; R and D Systems, Minneapolis, MN), anti-Nestin (1:250; Santa Cruz), anti-cleaved caspase 3 (1:250, Cell Signaling Technology, Boston, MA), anti-Doublecortin (DCX, 1:200; Santa Cruz), anti-Tbr2 (1:500; Millipore, Billerica, MA), anti-Ki67 (B56, 1:50; BD Biosciences, San Jose, CA), anti-Pecam-1/CD31 (BD Biosciences), anti-Prox1 (1:1,000; Sigma, St. Louis, MO; 1:500; Abcam, Cambridge, MA), and anti-Calbindin D28k (1:500; Millipore, Billerica, MA; CB-38a, 1:500; Swant, Switzerland). Species-specific AlexaFluor 488-, 594-, and/or 647-conjugated IgG (1:2,000; Invitrogen, Carlsbad, CA) were used for secondary antibodies in immunostaining experiments. 4′,6-Diamidino-2-phenylindole (DAPI) (Sigma, St. Louis, MO) or YO-PRO1 Iodine (1:1000, Invitrogen, Carlsbad, CA) were used for nuclear staining. For triple antibody staining, Donkey anti-goat Alexa-Fluor 647 (Nestin), anti-mouse AlexaFluro 568 (Sox2), and anti-rabbit AlexaFluro 488 (Cux2) secondaries (Invitrogen, Carlsbad, CA) were used. For Calbindin detection, citrate buffer antigen retrieval (pH 6.0; Thermo Scientific, Lab Vision Corporation, Fremont, CA) was performed.

Imaging and Quantification

DG morphology was assessed by Nissl staining using 0.1% cresyl violet solution (Sigma) and by DAPI staining and cell counts. The ontogenic profile of Cux2 expression was assessed by counting the total numbers of Cux2-positive nuclei per dentate blade and normalized over DAPI. For Nestin, Sox2, Cux2, GFAP, Tbr2, DCX, Calretinin, and Calbindin, a total of 50 parasagittal sections at 12 μm were obtained from C567Bl/6 wild type or Cux2-ires-Cre; R26r-tdtomato (see below) mice at P10, and P21. Parasagittal sections from 4 or 5 separate individuals were obtained throughout the entire DG starting from the midline to the lateral end of the DG. A total of 18–20 counting frames (100 μm × 100 μm) were randomly placed on the entire DG according to systematic-random sampling method (Mouton, 2002). The base of the counting frame was adjusted to align along the lower edge of the SGZ in order to avoid counting cells in the hilus region. The ontogenic profile of Cux2 expression was assessed by counting the total numbers of Cux2-positive nuclei per dentate blade and normalized over DAPI. Type 1 cells were defined by the combined expression of Nestin and Sox2 and presence of a Nestin- or GFAP-positive radial glial process. Images were captured using a Zeiss Z1 AxioObserver inverted fluorescence microscope with ×20 and ×63 objectives and apotome 2 (structured illumination). Confocal sections were imaged using a Zeiss 710 LSM microscope with ×40 objectives. Images were assembled using Photoshop CS2 (Adobe, San Jose, CA).

EdU Birth Dating

The dams were injected intraperitoneally with 30 mg/kg body weight of EdU (Invitrogen) on E17.5 and pup brains were dissected at P14 after perfusion with 4% PFA, followed by an overnight fix at 4°C and processing for cryosectioning. Sections were immunostained with Calbindin (Calb), Sox2, and EdU according to the manufacturer's instructions (Invitrogen). For postnatal analyses, pups were pulsed with 30 mg/kg EdU on P5 and sacrificed on P21. $Calb^+EdU^+$, $Sox2^+/EdU^+$, and total EdU^+ cells were counted in every 80 sections from the medial DG outward laterally. The Sox2 retention index was defined as the percentage of $Sox2^+EdU^+/EdU^+$. Some wild type P20 mice were pulsed with 30 mg/kg body weight EdU for 6 h to detect dividing SGZ progenitors. Brains were processed and sectioned as described above and stained for Nestin, Sox2, and Cux2 prior to EdU detection using the Click-It kit (Invitrogen).

Fetal DG Development

E14.5–18.5 fetal brains were fixed in ice-cold 4% PFA/0.1M PB overnight and processed for cryosectioning at 12 μm. Sections were blocked with 10% goat serum and incubated with either rabbit anti-Prox1 antibody (1:1,000; Sigma, St. Louis, MO) or mouse anti-Prox1 (1:500; Abcam) overnight at 4°C. Protein expression was detected using the appropriate HRP secondary antibodies and the Vectastain ABC kit (Vector Laboratories, Burlingame, CA) and 3.3'-Diaminobenzidine (DAB) staining (Dako Cytomation). $Prox1^+$ cells in the developing DG were counted in every 20 sections according to systematic-random sampling method (Mouton, 2002). Fractionator in Stereo Investigator (MBF Bioscience, Williston, VT) was used for cell counting. Total cell numbers were corrected by Abercrombie's method (Abercrombie, 1946) and standardized by body weight. For each group, 3–5 embryos from three different dams were analyzed. The data was evaluated using a two-tailed t-test with significance set at $P < 0.05$. Images of DAB-stained slides were captured using an upright bright field Zeiss microscope using an ERc 5s digital camera and Zen software.

Cux2 Fate Mapping

For the genetic fate labeling of Cux2-expressing NPs in the DG, we utilized a *Cux2-ires-Cre* driver line obtained from the Mutant Mouse Regional Resource Center. The strain designation is $B6(Cg)-Cux2^{tm1.1(Cre)Mull}/Mmmh$ (herein referred to as *Cux2-ires-Cre*), and contains an internal ribosome entry site (IRES) and nuclear localize Cre recombinase (NLS-Cre) targeted to the 3′ untranslated region (3′UTR) of the Cux2 locus (Fig. 7A). We genotyped this strain for the presence/absence of the Cre transgene using the following PCR primers: GTTATAAGCAATCCCCA-GAAATG and GGCAGTAAAAACTATCCAGCAA, which gives product of approximately 250 bp. For the reporter strain, we employed the *Rosa26-TdTomato*, designated $B6.Cg-Gt(Gt(ROSA)26Sor^{tm14}ROSA)$ $26Sortm14^{(CAG-tdTomato)HzetdTomato)}$ $^{Hze}/J$ (The Jackson Laboratory, Bar Harbor, ME). This strain expresses the Tomato transgene only upon Cre mediated excision of the floxed-translation Stop sequence in the *Rosa26* locus. The tomato fluorescence is bright and stable and has been validated in the mapping of Cre drivers during CNS development (Madisen et al., 2010). We genotyped for the presence/absence of the *Tomato*
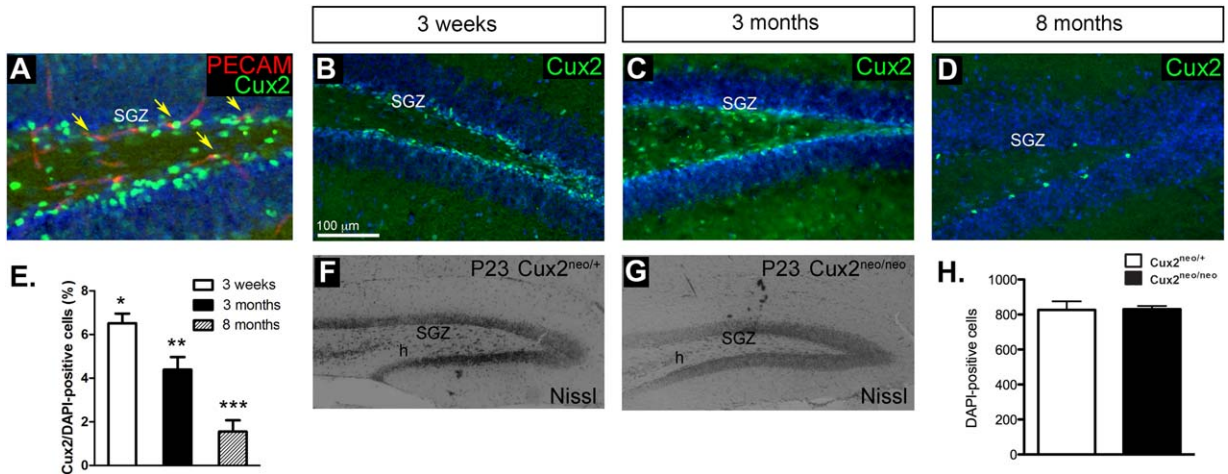
FIGURE 1. Cux2 is expressed in the SGZ and co-localizes with the vasculature. A: Niche vasculature stained with Pecam/CD31 (red) in and Cux2 (green) antibodies in 3-week-old (P23) mouse parasagittal sections across the hippocampus (arrows). B–D: Cux2 staining (green) in the SGZ at 3 weeks (B), 3 months (C), and 8 (D) months of age. E: Bar chart quantifying the significant decrease in Cux2 expression with age. Nissl staining reveals normal development of the DG in *Cux2*^{neo/neo} mice (G) compared to *Cux2*^{neo/+} littermate controls (F). H: Numbers of DAPI-positive cells were unchanged in the *Cux2*^{neo/neo} hippocampus compared to littermate controls ($P = 0.89$). Images were counterstained with DAPI. Abbreviations: DG, dentate gyrus; h, hilus; SGZ, subgranular zone. [Color figure can be viewed in the online issue, which is available at wileyonlinelibrary.com.]

transgene using the primers: TACGGCATGGACGAGCTGTACAAGTAA and CAGGCGAGCAGCCAAGGAAA, giving a 500 bp product. Allelism was determined using the primers: TCAATGGGCGGGGGTCGTT, TTCTGGGAGTTCTCTGCTGCC, CGAGGCGGATCACAAGCAATA, to amplify 250 bp wild type and 300 bp mutant bands. In fate-labeling experiments, the *Cux2-ires-Cre* line was mated with the *Rosa26r-tdTomato* to generate *Cux2-ires-Cre/+*; *Rosa26rtdTomato*^{/+} founders. Double heterozygotes were crossed with *Rosa26r*^{tdTomato/tdTomato} and brains from offspring were perfused-fixed at 7–10 days (P7–P10), 3 weeks (P21), 3 and 5 months of age. Brain tissue was cryoprotected and embedded in OCT, and sectioned at 14 μm parasagittally using a cryostat. Sections were subjected to immunostaining with antibodies described above, revealed by Alex Fluor 647 secondary antibodies (Invitrogen), and counterstained in DAPI. The resulting slides were imaged using a Zeiss AxioObserverZ1 equipped with Apotome 2 and ×20 and ×63 objectives.

RESULTS

Cux2 Was Expressed in the Progenitor Cell Niche of the SGZ

To investigate the role of Cux2 in the formation of neurons in the postnatal mouse brain, we first characterized the localization of Cux2 protein in parasagittal sections of the hippocampus. Since the neurogenic niche in the SGZ is bound by the vasculature (Palmer et al., 2000), we used a Pecam-1/CD31 antibody to identify blood vessels. Co-immunostaining with Cux2 antibody revealed that some Cux2-positive cells were found adjacent to the vasculature structure of the DG (arrows; Fig. 1A). Given that NPs similarly associate with the SGZ vasculature (Palmer et al., 2000), these findings suggested that Cux2 might be expressed in the neurogenic niche of the hippocampus.

We next profiled Cux2 levels in the hippocampus at various ages of the maturing mouse brain and found that Cux2 expression was greatest at 3 weeks of age (Fig. 1B), and decreased with age (Figs. 1B–E), until it was only minimally expressed in the occasional cell in the SGZ (Figs. 1D,E). Since the majority of postnatal neurogenesis in the mouse hippocampus occurs within the first few weeks of life (Kuhn et al., 1996; Liu et al., 2006), we focused our investigation 2–4 weeks of age when Cux2 levels were robust.

To determine whether Cux2 is required for normal hippocampal neurogenesis, we used a hypomorphic *Cux2*^{neo/neo} mutant mouse line (Iulianella et al., 2008). We previously reported that this *Cux2* mutation greatly attenuates Cux2 levels in the developing brain and displays a variable penetrance and expressivity of neurogenic phenotypes (Iulianella et al., 2008; Wittmann et al., 2014). Consistent with our previous findings, we observed no Cux2 immunoreactivity in the postnatal *Cux2*^{neo/neo} mutant hippocampus (Supporting Information Fig. S1). Most *Cux2*^{neo/neo} mutant offspring are viable and fertile, and thus can be used to investigate functions in the postnatal brain. Nissl staining showed that DG morphology appeared largely normal in *Cux2*^{neo/neo} mutant mice at P23 (Figs. 1F,G). Normal gross hippocampus formation was also supported by unchanged numbers of DAPI-positive cells in DG blades of the *Cux2*^{neo/neo} mutants (Fig. 1H). We observed no changes in
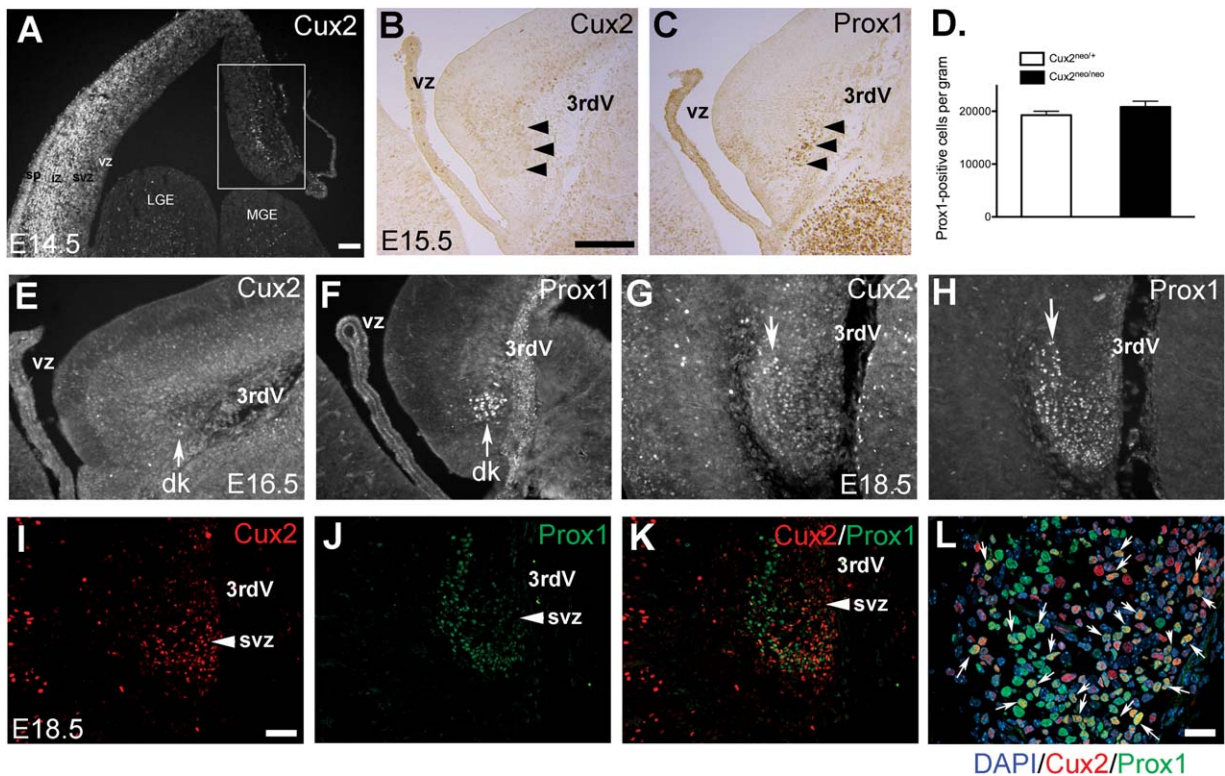
FIGURE 2. Cux2 expression during DG development. A: Cux2 immunofluorescence in the presumptive DG neuroepithelium of the medial telencephalon at E14.5. Boxed region identifies Cux2 staining in the presumptive hippocampus forming region of the forebrain. B, C: DAB immunostaining of Cux2 levels in the ingressing SVZ of the DG (B, arrow heads) relative to the immunostaining of a DG-specific marker, Prox1 in (C, arrow heads). D: There was no significant difference between $Cux2^{neo/+}$ controls and $Cux2^{neo/neo}$ mutants in the total numbers of Prox1$^+$ cells in the forming DG region at E16.5. E, F: Cux2 and Prox-1 immunofluorescence staining in the developing DG at E16.5. Cux2 was weakly expressed in the dk at E16.5 (E), relative to strong Prox-1 staining (F). G, H: Cux2 (G) and Prox1 (H) immunofluorescence staining in the SVZ of the developing DG at E18.5. Arrowheads in (G) and (H) identify the developing DG germinal matrix. I, L: Cux2 and Prox1 co-staining in the developing DG at E18.5. I: Cux2 expression (green) in the SVZ of the DG primordium adjacent to the 3rdV. J: Prox1 staining (green) in the newly forming granule cells of the fetal DG. K: Cux2 (red) and Prox1 (green) staining in the DG primordium. L: High magnification (63×) view of Cux2 (red) and Prox1 (green) co-staining (arrows) in nascent granule cells (arrows). Nuclei were visualized with DAPI staining. Scale bars: A,B: 100 μm; I: 50 μm; L: 25 μm. Abbreviations: DG, dentate gyrus; dk, dentate knot; IZ, intermediate zone; LGE, large ganglionic eminence; MGE, medial ganglionic eminence; sp, subplate; IZ, intermediate zone; SVZ, subventricular zone; VZ, ventricular zone; 3rdV, third ventricle. [Color figure can be viewed in the online issue, which is available at wileyonlinelibrary.com.]

Cleaved Caspase-3 staining in $Cux2^{neo/neo}$ mutant vs. $Cux2^{neo/+}$ littermate controls, indicating *Cux2* loss did not alter apoptosis levels in the hippocampus (data not shown).

Cux2 Was Expressed During DG Morphogenesis

Since Cux2 plays a role in neural development in the spinal cord and cortex (Iulianella et al., 2003, 2008, 2009; Zimmer et al., 2004; Cubelos et al., 2008a), we examined the distribution of Cux2 in the presumptive DG-forming region of the medial cortex. The DG originates from the ventricular region of the medial telencephalon from E14.5 onwards. We observed a localized expression of Cux2 protein in this region by fluorescence immunohistochemistry at E14.5 (Fig. 2A, boxed region). As development progresses, both morphogenetic movements and proliferation causes the displacement of the developing DG neuroepithelium toward the inner core of the medial telencephalon. Prox1 is a transcription factor that is expressed in granule cell neurons from the onset of their formation in the fetal DG and continues in post-mitotic gcl neurons of the adult hippocampus (Lavado and Oliver, 2007; Steiner et al., 2008). We therefore used Prox1 as a marker for developing DG neuroepithelium in alternative sections to Cux2 staining for morphological comparisons. Cux2$^+$ cells were detected in the E15.5 DG neuroepithelium by DAB immunostaining, which also expressed Prox-1 (arrowheads, Figs. 2B,C). We found that Cux2 expression coincided with Prox1 in the dentate germinal region called the dentate knot at E16.5, although Cux2 levels were mosaic and much lower relative to Prox1 (Figs. 2E,F). By E18.5, Cux2 staining continued to be mosaic
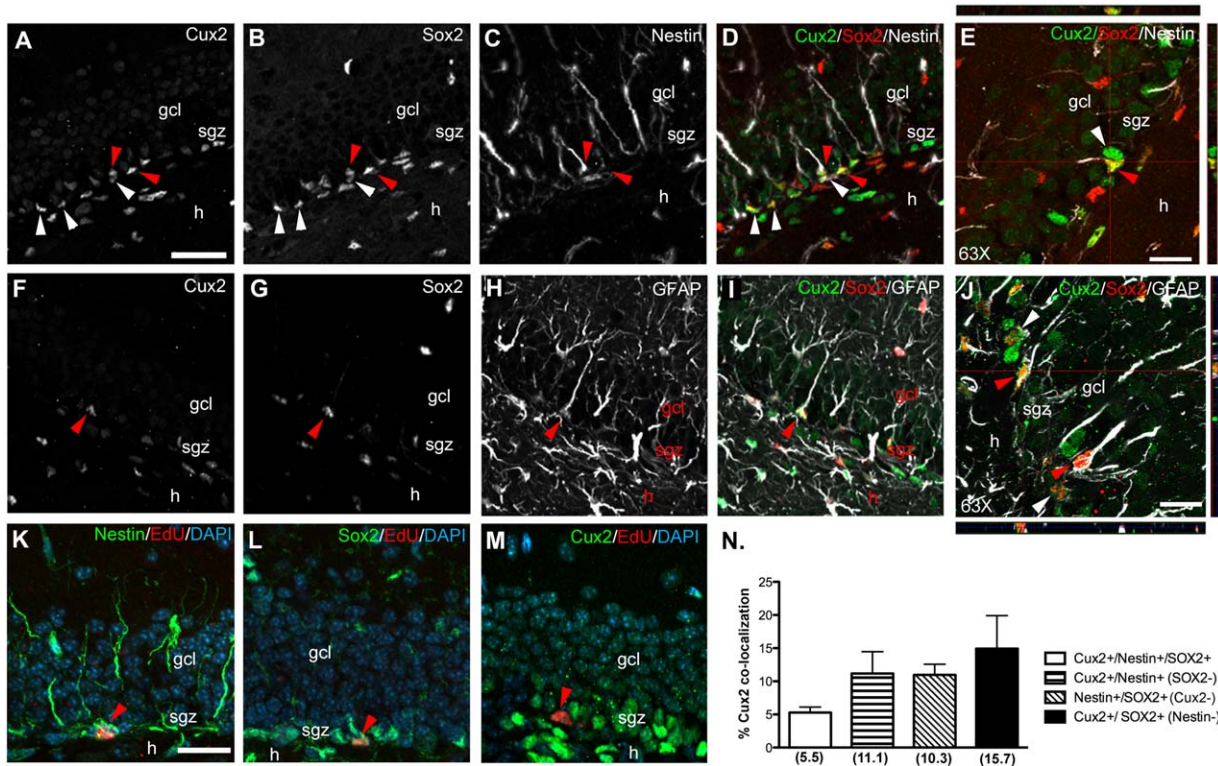
FIGURE 3. Cux2 is expressed in Nestin, GFAP, and Sox2 positive radial glia. A–E: Cux2 (A) co-localization in Sox2 (B) and Nestin (C) positive cells in the SGZ at P21. D: Cux2 (green), Sox2 (red), and Nestin (white) co-localization in Type 1 radial glia (red arrowhead). Cux2 was also expressed in Sox2$^+$ but Nestin-negative Type 2 cells (white arrowhead). E: High magnification (63×) Z-stack image of Cux2 (green) co-localization in a Sox2 (red) and Nestin (white) double-positive radial glia Type 1 progenitor (red arrowhead). Cux2 was also co-expressed in Sox2$^+$/Nestin$^-$ Type 2 cells (white arrowhead). F–K: Cux2 (F) co-localization in Sox2 (G) and GFAP (H) positive cells in the SGZ. I: Cux2 (green), Sox2 (red), and GFAP (white) co-localization in Type 1 radial glia (red arrowhead). K: High magnification (63×) Z-stack image of Cux2 (green) co-localization in a Sox2 (red) and GFAP (white) double-positive Type 1 progenitor possessing a radial glia (red arrowhead). Cux2 was also co-expressed in Sox2$^+$/GFAP$^-$ Type 2 cells (white arrowhead). K–M: EdU (red) co-staining with Nestin (green, arrowhead, K), and Sox2 (green, arrowhead, L). Cux2 (green) was not detected in dividing EdU$^+$ SGZ cells (red, arrowhead, M). N: Chart summarizing Cux2 expression in Type 1 (Nestin$^+$/Sox2$^+$) and Type 2 (Sox2$^+$/Nestin$^-$) cells at P21. A greater proportion of Cux2 expression was detected in Type 2 (15.7%) cells vs. Type 1 cells (5.5%). Cux2 was also co-localized in Type 3 cells (neuroblasts) and nascent neurons (see Fig. 4). Scale bars: A and K, 25 μm; E and J, 8 μm. Abbreviations: h, hilus; gcl, granule cell layer; SGZ, subgranular zone. [Color figure can be viewed in the online issue, which is available at wileyonlinelibrary.com.]

and was most intense in the inner core of the forming DG blade and SVZ, while Prox1 was highly expressed throughout the developing DG (arrow, Figs. 2G,H). We confirmed Cux2 expression in Prox1$^+$ nascent granules cells in co-immunostaining experiments (Figs. 2K–L). Interestingly, while there is significant overlap between Cux2 and Prox1 expression in the DG primordium (Figs. 2K,L(arrows)), they broadly segregate to two domains, with Cux2 labeling SVZ progenitors as well as nascent granule cells, and Prox1 being restricted to newly forming granule neurons (Figs. 2I–K). This suggested that Cux2 expression in the medial forebrain labeled SVZ progenitors fated to form the DG granule cells.

To evaluate a role Cux2 in DG formation, we examined the numbers Prox1$^+$ cells in the dentate knot of *Cux2$^{neo/neo}$* mutants using serial frontal sections of the E15.5 DG. The *Cux2$^{neo/neo}$* mouse mutant is a hypomorph showing little or no Cux2 expression in the developing brain (Iulianella et al.,

2008), olfactory epithelium (Wittmann et al., 2014), or hippocampus (Supporting Information Fig. S1). We did not detect any significant changes in Prox1 numbers in *Cux2$^{neo/neo}$* mutants in comparison to their *Cux2$^{neo/+}$* littermate controls (Fig. 2D), consistent with the normal DG morphology in the adult mutant brain. Thus, Cux2 was expressed in the Prox1$^+$ DG neuroepithelium at the onset of its morphogenesis, but was dispensable for DG formation.

Cux2 Is Expressed in Neural Progenitors in the SGZ of the Hippocampus

Cux2 was expressed in the early germinal neuroepithelium of the DG as well as the SGZ in the postnatal brain (Figs. 1 and 2). Both these regions contain NPs, including Type 1 cells, which are characterized by a radial glial process and the expression of Nestin, Sox2, and GFAP (Seri et al., 2004;

J.	DCX[1]	CalR[1]	Tbr2
% Cux2 co-localization	19.6 +/- 2.8	44.6 +/- 4.2	3.9 +/- 1.0
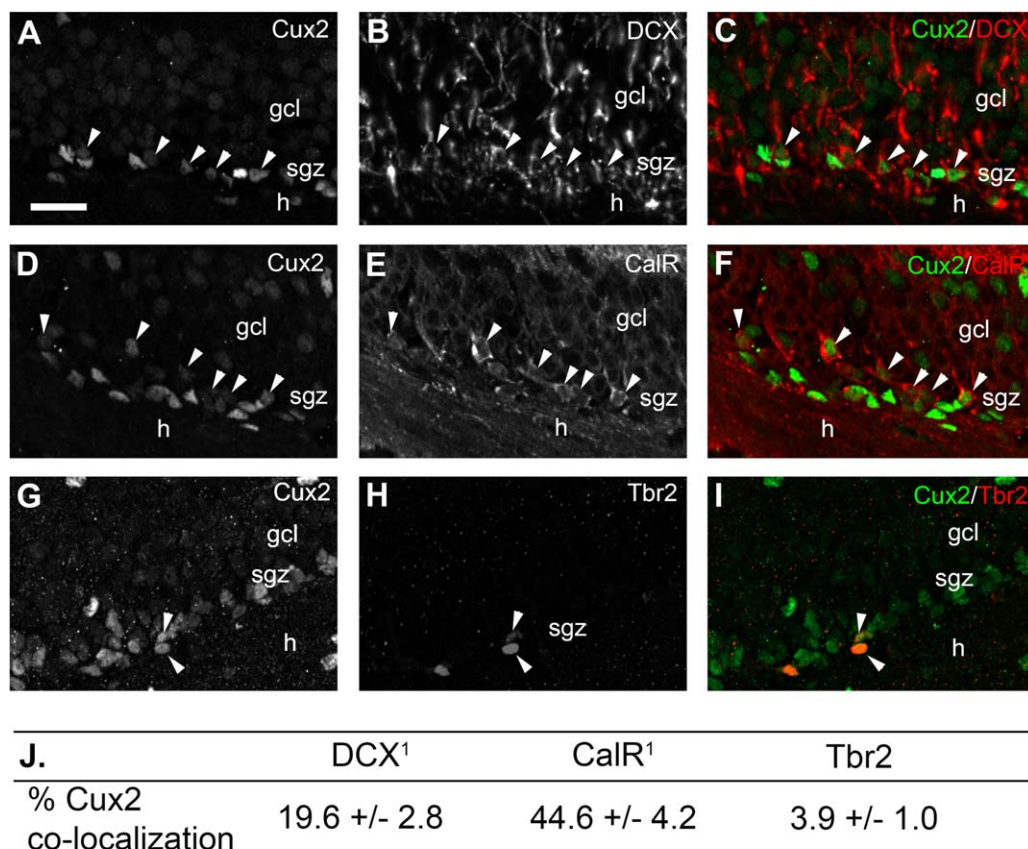
[1] Weak Cux2 expression in co-localized cells

FIGURE 4. Cux2 is expressed in neuroblasts and immature granule neurons. A–C: Cux2 (A, C, green) staining in DCX[+] neuroblasts (B, C, red) in the SGZ at P21. C: The Cux2/DCX co-stained cells (arrowheads) typically displayed lower levels of Cux2 protein relative to adjacent SGZ cells. D–F: Cux2 expression (D, F, green) in Calretinin^{+} immature neurons (E, F, red) arrowheads). F: Co-stained cells expressed lower levels of Cux2 (arrowheads). G–I: Limited Cux2 expression (G, I, green) in Tbr2^{+} transit amplifiers (H, I, red; arrowhead). J: Quantification of Cux2 co-localization with DCX, CalR, and Tbr2. Most Cux2^{+} (44.6%) cells in the SGZ were CalR^{+} immature neurons. Cux2 co-staining in DCX[+] and CalR^{+} cells displayed low levels of Cux2 expression. Scale bar: A, 25 μm. Abbreviations as in Figure 3; CalR, Calretinin. [Color figure can be viewed in the online issue, which is available at wileyonlinelibrary.com.]

Kriegstein and Alvarez-Buylla, 2009). We asked whether Cux2 was expressed in Type 1 NPs by immunostaining for Nestin, Sox2, and GFAP. Cux2 was expressed in the nuclei of SGZ cells that possessed a Nestin[+] radial glia and also expressed the stem cell marker Sox2 (red arrowhead, Figs. 3A–E). High-resolution Z-stack imaging revealed Cux2 co-staining in Nestin[+]/Sox2^{+} radial glia characterized by a typical Type 1 pyramidal morphology (red arrowhead, Fig. 3E). Cux2 was also detected in Type 2 cells, which express Sox2, but lack a radial glia and markers for astroglial stem cells (white arrowhead, Figs. 3D,J). We confirmed Type 1 expression by immunostaining for GFAP to label astroglial progenitors in the SGZ (Rickmann et al., 1987; Liu et al., 2010). We observed Cux2 co-staining in GFAP[+]/Sox2^{+} cells characterized by radial processes spanning the DG from SGZ upward into the gcl (red arrowhead, Figs. 3F–J). When we sampled the entire DG and quantified our co-localization data we determined that 5.5% of all Cux2^{+} cells in the SGZ possess radial glia and co-expressed both Sox2 and Nestin (Fig. 3N). We observed a greater proportion (15.7%) of Cux2^{+} cells were Type 2 cells that expressed Sox2 but lacked Nestin expression and radial glia (Fig. 3N; white arrowheads Figs. 3A–J). We also found that the highest Cux2/Sox2 co-localization occurred in DG sections closer to the midline (Supporting Information Fig. S2).

We then asked whether Cux2 co-localized to proliferating SGZ progenitors, identified by a short 6 h pulse of EdU. These EdU^{+} cells were indeed dividing progenitors by virtue of co-expression with Nestin (Fig. 3K) and Sox2 (Fig. 3L). However, they did not express Cux2 (Fig. 3M), which was distributed in adjacent SGZ cells. We confirmed this result by using the proliferative maker Ki67 and again found no evidence of Cux2 labeling in dividing SGZ cells (data not shown). These findings demonstrate that Cux2 was expressed in non-dividing Type 1 and Type 2 progenitors lining the SGZ of the neonatal mouse hippocampus.

Cux2 Is Expressed in Neuroblasts and Nascent Neurons

We next evaluated the distribution of Cux2 protein in more differentiated cell types in the DG, including newly forming neurons, neuroblasts, and transit amplifiers. To identify neuroblasts (Type 3 cells), we used DCX immunostaining in 3-week-old brains (P21). We noted extensive Cux2 co-localization with DCX$^+$ nascent neurons that appeared to migrate away from the SGZ into the gcl (arrowheads, Figs. 4A–C). Interestingly, Cux2$^+$/DCX$^+$ cells typically displayed lower Cux2 levels relative to their Cux2$^+$ neighbors that lacked DCX expression (Fig. 4C). We also used Calretinin staining to identify newborn granule cells in the neonatal SGZ (Brandt et al., 2003). As with DCX, we observed extensive Cux2 localization in Calretinin$^+$ cells migrating away from the SGZ (arrowheads, Figs. 4D–F). Again, most Cux2$^+$/Calretinin$^+$ co-localized cells displayed reduced Cux2 levels relative to the Cux2$^+$ cells in the SGZ/hilar boundary (Fig. 4F). Lastly, we profiled Cux2 distribution in Tbr2$^+$ transit amplifiers (Type 2b cells) and found limited co-expression in the SGZ (arrowheads, Figs. 4G–I). We found that 44.6% of Cux2-expressing cells (mostly low expression) were Calretinin$^+$ nascent neurons, while a considerable co-localization was also noted with DCX (19.6%; Fig. 4J). Few Cux2$^+$/Tbr2$^+$ cells were observed, although this was likely due to the normally low levels of this factor in the SGZ (Fig. 4J). We did not detect any Cux2 expression in PDGFRα-positive oligodendroctyes (data not shown), suggesting its expression coincided with hippocampus neurogenesis, similar to its role in the embryonic spinal cord and cortex (Zimmer et al., 2004; Cubelos et al., 2008a; Iulianella et al., 2008). Taken together, these findings suggest that most cells expressing Cux2 in the neonatal hippocampus were neuroblasts and their immediate Type 1 and Type 2 progenitors.

Fate-Map of Cux2-Expressing Cells Revealed the Outside-In Formation of the DG

At postnatal stages, Cux2 expression was primarily restricted in a subset of Nestin and Sox2 double-positive NPs (Fig. 3). Since Nestin$^+$/Sox2$^+$ NPs give rise to gcl neurons (Bonaguidi et al., 2011; Suh et al., 2007), we expected that Cux2-expressing NPs would also generate gcl neurons. To fate-map Cux2-expressing cells in the hippocampus, we utilized a Cux2-ires-Cre line that has an IRES-nuclear localized Cre cassette inserted in the 3'UTR of the Cux2 locus (Materials and Methods). We mated this Cre driver to a R26r-tdTomato transgenic reporter to generate a *Cux2-ires-Cre; R26r-tdTomato* line that expressed tdTomato fluorescent protein upon a Cre-mediated excision driven by the Cux2 locus (Supporting Information Fig. S3). We found that the hippocampus was highly labeled by red fluorescent protein (Supporting Information Figs. S3B–G). At 10 days after birth (P10), when postnatal neurogenesis is ongoing, Tomato$^+$ cells localized in clusters in the SGZ and in a thin band of cells in the outer-most gcl (arrow, Supporting

Information Figs. S3B,C). At 3 weeks of age (P21), Tomato labeling progressed to encompass more granule cells of the DG (arrowhead, Supporting Information Figs. S3D,E), until by 5 months of age most granule cells were Tomato$^+$, with limited labeling in the SGZ (Supporting Information Figs. S3F,G). Because low levels of Cux2 were expressed in gcl neurons (Supporting Information Figs. S2B,F), we examined whether Tomato$^+$ cells co-expressed Cux2, and confirmed co-localization (arrows, Supporting Information Fig. S4). The co-localization was imperfect, which is expected given the nature of genetic recombination strategy using Cre recombinase (see discussion). Altogether, these findings revealed that Cux2 activity mapped the formation of gcl neurons in an outside-in manner, but did not result in significant SGZ labeling.

Cux2 Fate-Mapped Cells Were Calbindin-Positive DG Granule Cell Neurons

The temporal profile of Cux2-ires-Cre; R26r-tdTomato labeling suggested that Cux2$^+$ progenitors generated gcl neurons in an outside-in manner reflecting the dynamic morphogenesis of the DG [Supporting Information Fig. S3 (Altman and Bayer, 1990b)]. At P21, Cux2 was expressed in two distinct domains: a Cux2^{high} region in the SGZ comprising of progenitors and neuroblasts, and a Cux2^{low} expression domain in the outer regions of the gcl (Supporting Information Figs. S2 and S4 and Fig. 5B). When we examined Cux2 expression in the P21 Cux2-ires-Cre; R26r-tdTomato fate mapped cells, we found that nearly all of the Cux2^{low} cells were Tomato$^+$ gcl neurons (92.4 ± 0.4%; arrow, Figs. 5A–C). In contrast, very few Cux2^{high} cells in the SGZ were Tomato$^+$ (1.5 ± 0.1%). Using immunohistochemistry we confirmed most of the Tomato$^+$ outer gcl cells were mature Calbindin$^+$ granule neurons (85.0 ± 3.6%; Figs. 5D–F). Since Type 1 progenitors are thought to differentiate into mature neurons by transitioning through a neuroblast stage, we next examined DCX immunostaining in the Cux2-ires-Cre fate-mapped DG. We found a complementary pattern of expression of DCX in the SGZ and inner edge of the DG, with DCX$^+$ cells localizing to the tomato$^-$ SGZ at P21 (Figs. 5G–I). The occasional co-staining of DCX in Tomato$^+$ fate-mapped cells was observed in the SGZ (arrowhead, Fig. 5I). Interestingly, at P10 DCX expression diffusely co-localized with Tomato$^+$ tissues in the outer-most layer of the developing gcl (Supporting Information Figs. S5A–C). At this developmental period, we also observed weakly fluorescent tomato$^+$ cells in the SGZ that co-stained with Calretinin, a marker for newborn immature neurons (arrowheads, Supporting Information Figs. S5D–F). This is consistent with the activity of Cux2 in early-born granule cell neurons from fetal stages onwards (Fig. 2). Thus, the Cux2 fate-mapping studies primarily reflect neurogenesis in the hippocampus at perinatal stages, which contributes to granule cells in the outer blades of the DG.

To determine Cux2 fate-mapped cells were primarily gcl neurons, we examined the distribution of the astroglial marker GFAP, and found a mutually exclusive staining pattern for
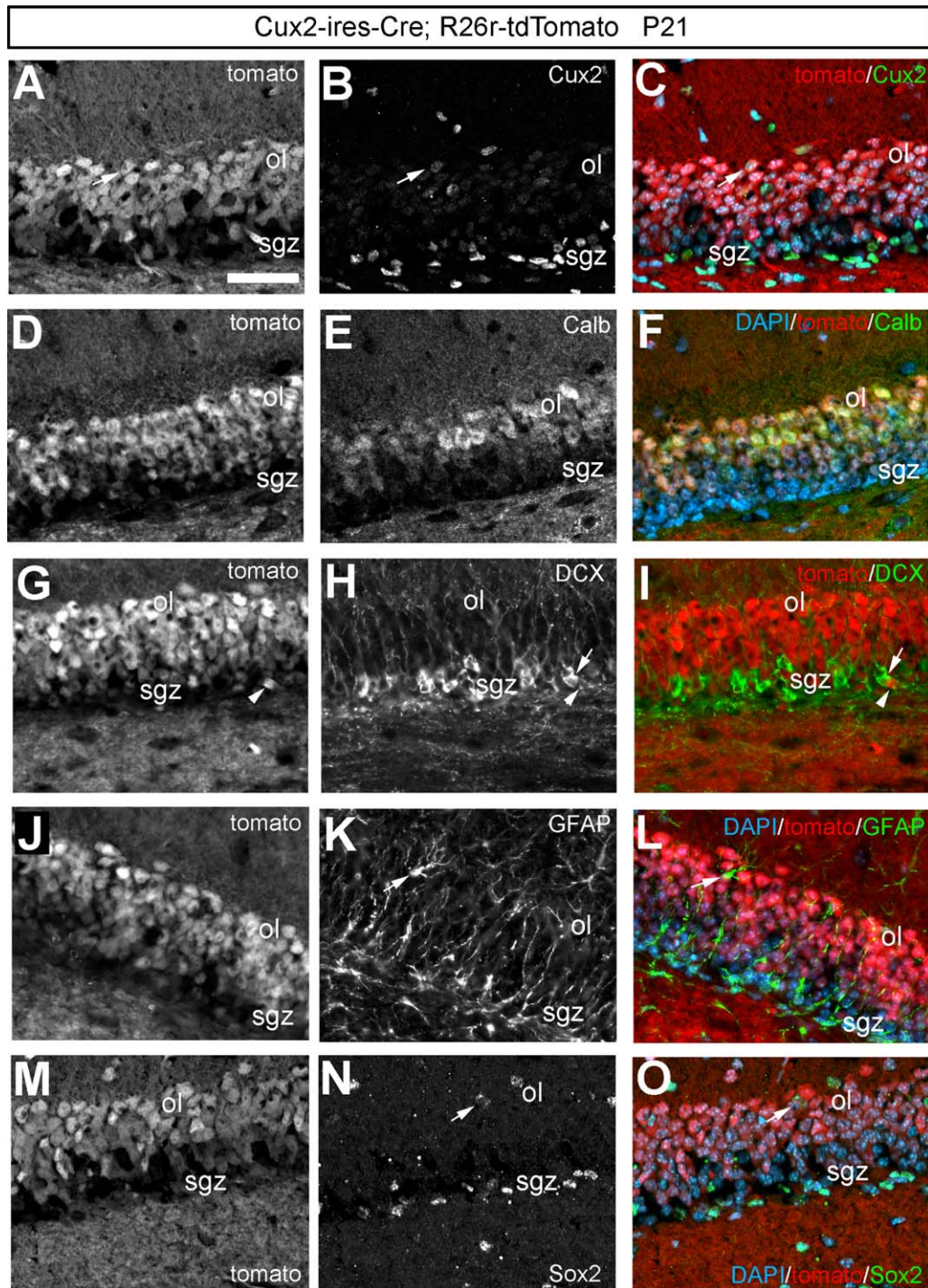
FIGURE 5. Cux2 fate-mapped cells were Calbindin-positive mature gcl neurons. A–C: Cux2-cre; tdTomato fate mapped cells in the DG of P21 mice. C: Tomato⁺ fate-mapped cells showed limited or no localization with high Cux2⁺ expressors, in the SGZ and instead localized to outer layer DG cells expressing low Cux2 levels (arrow in B, C). D–F: Tomato fate-mapped cells localized to Calbindin-expressing gcl neurons. G–I: Tomato fate-mapped cells of the P21 DG did not localize with DCX⁺ neuroblasts. H, I: Arrow identifies a tomato⁺ cell in the SGZ that did not express DCX (arrowhead). J–L: Tomato fate-mapped cells of the P21 DG did not localize with GFAP⁺ astroglia. K, L: Arrow identifies a GFAP⁺ astrocyte in the outer layer of the DG that was negative for tomato. M–O: Tomato⁺ cells did not co-localize with Sox2 in the SGZ or occasional Sox2⁺ cell in the outer layer of the DG (arrow). Scale bar: A, 50 μm. Abbreviations: Calb, Calbindin; ol, outer layer of the DG; SGZ, subgranular zone. [Color figure can be viewed in the online issue, which is available at wileyonlinelibrary.com.]
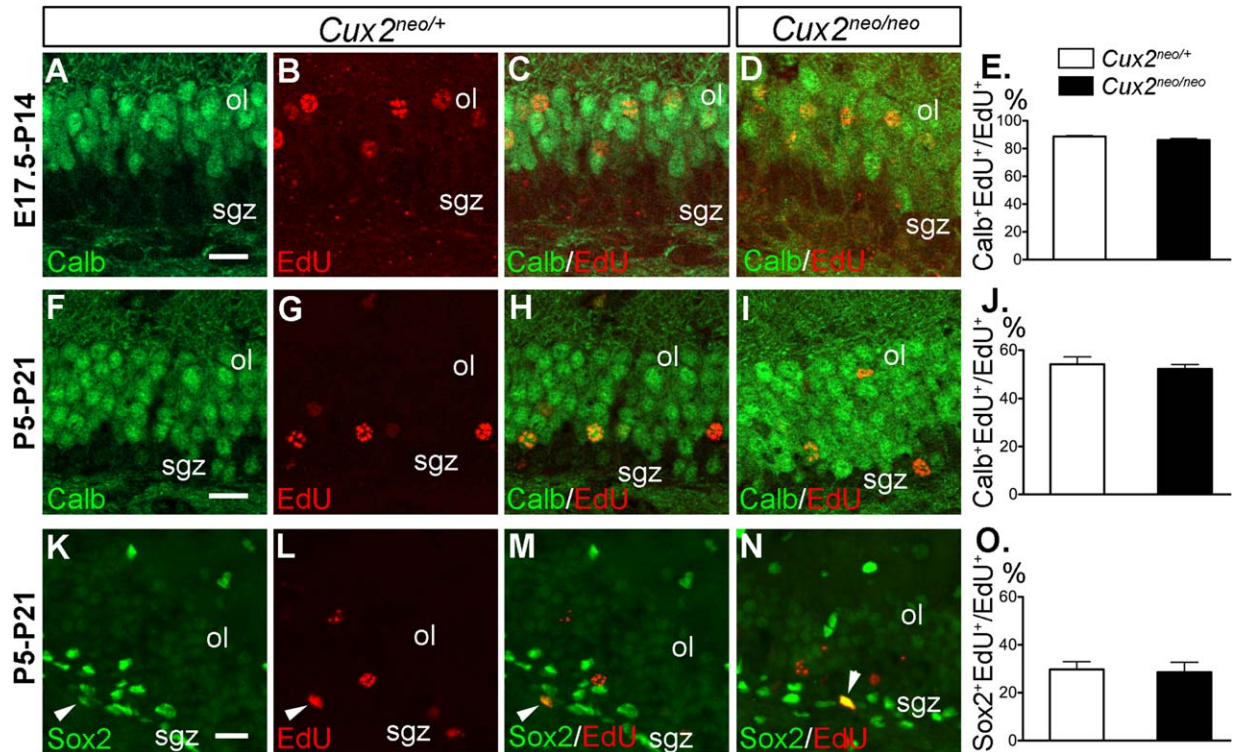
FIGURE 6. Birth dating analysis in *Cux2neo/neo* mutants. A–E: EdU was injected at E17.5 and the embryos (*n* = 5 for each group) were analyzed at P14 by immunohistochemistry using anti-Calb antibody (green) and EdU staining (red). A–C: EdU pulsing at E17.5 revealed labeling of mature Calb$^+$ neurons in the outer layer of the DG. E: The percentage of cells double positive for Calb and EdU (Calb$^+$EdU$^+$) in the total EdU-positive cells (EdU$^+$) were not significantly different between *Cux2neo/+* controls (C) and *Cux2neo/neo* mutants (D) (*P* = 0.09). F–I and K–N: EdU was injected at P5 and the analyses were done at P21 (*n* = 4 for each group). Pulsing at P5 labeled deeper regions of the dentate blade and resulted in EdU co-staining with Calb (F–I) and Sox2 (K–N). J: The percentage of Calb$^+$/EdU$^+$ cells over total EdU$^+$ was comparable between controls and mutants (*P* = 0.61). O: The percentage of Sox2$^+$/EdU$^+$ in the total EdU$^+$ pool (retention index) was similar between controls and mutants (*P* = 0.83). Scale bars: 20 μm. Abbreviations as in Figure 3; Calb, Calbindin. [Color figure can be viewed in the online issue, which is available at wileyonlinelibrary.com.]

GFAP and Tomato$^+$ cells (Figs. 5J–L). This was also observed for GFAP-positive astrocytes located within the gcl of the DG, which did not localize to Tomato$^+$ positive cells (arrow, Figs. 5K,L). Lastly, we confirmed that Tomato$^+$ cells were not Sox2$^+$ NPs (Figs. 5M–O). Altogether, our P10 and P21 Cux2 fate mapping experiments demonstrate that Cux2$^+$ progenitors gave rise to neuroblasts that transitioned to mature Calbindin$^+$ granule cells populating the DG in an outside-in manner

Cux2 Was Dispensable for Differentiating DG Granule Cell Neurons

To evaluate a role for Cux2 in the differentiation of gcl neurons in the DG, we used EdU birth dating studies in *Cux2neo/neo* mutants. We focused on two stages to label the outside-in formation of the DG. An EdU pulse at E17.5 would reveal granule neurons that arise from the primary germinative matrix in the developing DG while a pulse at P5 will show the granule neurons that are generated from the secondary migration of SVZ precursors (Fig. 7A). The resulting DG were harvested at P14 and P21,

respectively, and stained for EdU and Calbindin to reveal the outside-in formation of the DG. As expected, the E17.5 pulse labeled Calbindin-positive granule neurons populated the outer layer of the DG (Figs. 6A–C), while P5 labeled Calbindin-positive neurons located in deeper regions of the DG blade. The loss of *Cux2* did not significantly impact gcl differentiation at E17.5 (Figs. 6D,E) and P5 (Figs. 6I,J). We also quantified the EdU retention index in Sox2-positive SGZ progenitors at the P5 (arrowhead, Figs. 6K–N), which is a measure of the quiescent progenitor pool fraction. We were interested in examining this population because Cux2 extensively co-localized with Sox2 in the SGZ (Fig. 3) and needed to determine whether the lack of an effect on Calbindin$^+$ cells was due to a compensatory effect in the progenitor pool. We noted no changes in the number of Sox2$^+$ progenitors that retained EdU in the *Cux2* mutants, indicating that the *Cux2* loss did not overtly alter the development of the SGZ progenitors (Figs. 6N,O). Taken together, our findings showed that Cux2 was expressed in a subset of Type 1 progenitors during DG development that gave rise to mature granule cells of the hippocampus in an outside-in manner, reflecting the
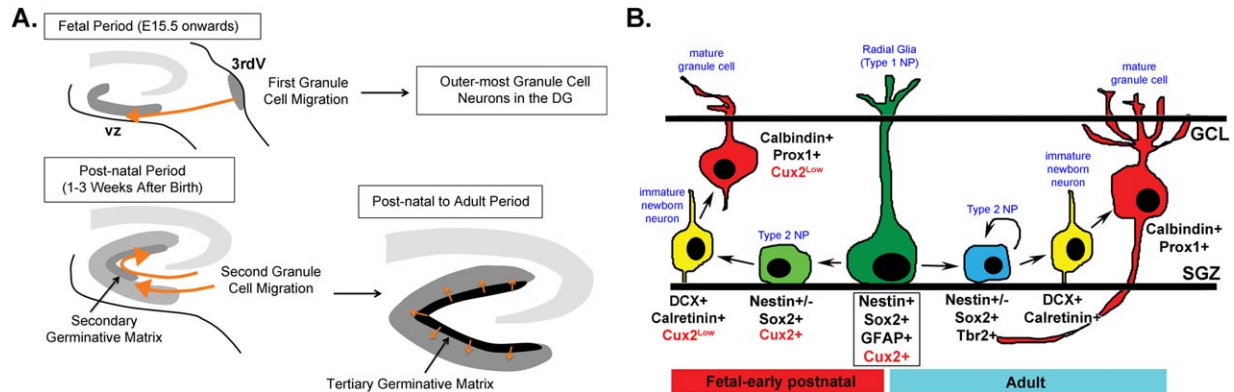
FIGURE 7. Model of DG morphogenesis and Cux2 activity in perinatal hippocampus progenitors. A: Schematic of DG morphogenesis in the rodent brain. The first wave of granule cell precursors arises at fetal stages (E15.5 in the mouse) and migrates away from the 3rd ventricle (3rdV) region to populate the growing subventricular (SVZ) dentate matrix in the medial region of the telencephalon. These cells are fated to give rise to the outer-most granule cell neurons. As DG development continues within the first few weeks of life, a second germinative matrix forms deep within in the SVZ of the medial telencephalon. This is the dentate knot. *Cux2* activity is high at these early stages of DG morphogenesis. As the animal progresses to adulthood, the tertiary germinative matrix forms and becomes populated with long-lived multipotent NPs. This region is the SGZ that houses Type 1 cells capable of giving rise to nascent neurons well into adult life. B: Model of Cux2 localization is a subset of Type 1 progenitors that originate in the dentate germinal regions at fetal stages and persists to the first weeks of life. This is a transitory progenitor that is transiting from a Type 1-like Nestin+/GFAP+/Sox2+ radial glia to a Sox2+ Type 2 cell, which lack a radial process and astroglial markers. Cux2 was also detected in DCX$^+$ neuroblasts (Type 3 cells) and immature newly formed granule cells identified by Calretinin expression. Fate mapping of Cux2-expressing progenitors revealed labeling of Calbindin-positive DG cells, and not SGZ progenitors, suggesting that the Cux2$^+$ progenitor does not self-renew and directly generates granule cells. Abbreviations as in Figure 3. [Color figure can be viewed in the online issue, which is available at wileyonlinelibrary.com.]

dynamic morphogenesis of this structure. However, we also noted that *Cux2* loss did not overtly affect DG morphogenesis or the differentiation of granule neurons, suggesting possible genetic compensatory mechanisms.

DISCUSSION

Neurogenesis is a highly regulative process that has implications for the limited regenerative abilities of the brain. Much attention has been focused on the elucidation of the mechanisms governing the birth of neurons in two regions of the adult brain: the SVZ of the lateral ventricle and the SGZ of the hippocampus. Although progress has been made, our knowledge of the neurogenic factors and the origin of the progenitor cell types in the postnatal mammalian brain remain rudimentary. Here, we report that in the postnatal hippocampus the transcription factor Cux2 was expressed in Nestin / Sox2 double-positive Type 1 NPs, Type 2 Sox2$^+$/Nestin$^-$ cells, DCX$^+$ neuroblasts, and Calretinin$^+$ nascent neurons in the SGZ. For the Type 1 and 2 cells, Cux2 principally localized within non-dividing progenitors. A lower level of Cux2 expression was seen in the maturing Calbindin$^+$ granule cells of the outer region of the DG blades in the neonatal brain. In the fetal brain, Cux2 was expressed in the SVZ of the medial forebrain corresponding to the germinal matrix of the developing DG, where it associated with Prox1$^+$ early born granule cells.

Thus Cux2 expression is associated with the generation of nascent granule cells from the earliest stages of hippocampus morphogenesis to within the first weeks of life. However, the maturation of the DG was associated with a progressive reduction of Cux2 staining in the SGZ. This is consistent with the observation that the majority of Cux2 cells expressed markers of nascent neurons and neuroblasts. As we noted in other regions of the developing nervous system, the expression and function of Cux2 seems to be specific for the genesis of newborn neurons (Iulianella et al., 2008; Wittmann et al., 2014).

We also revealed that Cux2-expressing NPs fate map the gcl in an outside-in manner. To our knowledge this is the first genetic demonstration that the DG of the hippocampus is patterned in outside-in manner and confirms the observations from classic birth-dating studies on DG morphogenesis (Altman and Bayer, 1990a,b). Our findings support a model of Cux2 activity in an early perinatal pool of non self-renewing SGZ progenitors that contribute to granule neuron production in the primary and secondary germinal matrices preceding the establishment of longer-lived Type 1 cells in the SGZ (Fig. 7).

The morphogenesis of the DG is highly dynamic and complex. The gcl is the most anatomically prominent region of the DG, and granule cells arise from multiple germinal sources during development. Initially, granule cell precursors arise from the ventricular region adjacent to the future 3rd ventricle of the medial region of the telencephalon at early fetal stages in rodents. This is known as the primary germinal matrix for granule cell neuron production. These precursors migrate inward to seed what will become the secondary germinal

matrix that becomes displaced in the subventricular region of the dentate primordium (Fig. 7A) (Altman and Bayer, 1990b). The granule cells that originate from these regions populate the outer portion of the dentate blade. We observed Cux2 expression in both these germinal sources, and our *Cux2-ires-Cre; R26r-tdTomato* fate-mapping studies showed dentate blade labeling in an outside-in manner (Fig. 5 and Supporting Information Figs. S3 and S5). This phenomenon reflects both the formation and progressive maturation of the DG at perinatal stages (Altman and Bayer, 1990a). Shortly after birth, a third germinal region in the inner lining of the developing DG replaces the secondary germinal matrix. This is the SGZ and supplies newborn gcl neurons within the first few weeks of life. Although the DG is not layered, there is a clear anatomical segregation as to the birth order of the gcl neurons, with the oldest neurons occupying the outer edge of the dentate blade and the newer neurons populating the deeper recesses of the blade.

Interestingly, the outside-in formation and maturation of the DG blade is reminiscent of the layered formation of the neocortex, which occurs in an inside-out manner. It is not known whether the stratified organization of hippocampal neurogenesis is genetically regulated in a similar fashion to the neocortex. Given the importance of Cux2 in layer specification in the neocortex (Nieto et al., 2004; Zimmer et al., 2004; Cubelos et al., 2008a; Franco et al., 2012; Guo et al., 2013), it is tempting to speculate that it also plays a role in patterning more evolutionarily ancient structures in the brain such as the archicortex, which includes the hippocampus. Our fate labeling studies using *Cux2-ires-Cre; R26r-tdTomato* mice revealed that Cux2-positive progenitors appear to give rise to clusters of gcl neurons within the first weeks of life. These labeled cells accrue in the DG in an outside-in manner, progressively filling the dentate blade such that by adult stages almost the entire DG expresses the *tomato* reporter gene, with the notable exception of most of the SGZ. This suggests that Cux2 acts in both the secondary and tertiary germinative matrices to progressively label almost all gcl neurons.

Nearly all the Cux2-fate mapped cells were mature Calbindin$^+$ granule cells, with surprisingly limited or no labeling of progenitor cells or astroglia. In contrast, the highest level of Cux2 protein staining occurred within progenitor populations and neuroblasts of the SGZ. This included Nestin$^+$/Sox2$^+$ positive radial glial cells, as well as Sox2$^+$/Nestin$^-$ in the SGZ of the neonatal brain. Yet limited co-staining was observed in Cux2-Tomato fate-mapped cells in the SGZ. There are three possibilities that can explain this discrepancy. The first concerns the observed low levels of Cux2 staining in the maturing granule cells of the DG. These cells are highly (85%) co-localized with tomato levels in the gcl, and can account for the activation of Cre recombinase leading to tomato fluorescence. Recently, a similar phenomenon was seen in a Neurod1-Cre fate mapping study in the hippocampus (Aprea et al., in press). While Neurod1 expression localized to the SGZ, extensive reporter labeling was observed in the mature granule cells of the DG. This was attributed to possible low levels of Neu-

rod1 (and therefore Cre) expression in the gcl that were not detectable by immunostaining or mRNA in situ hybridization. We however observed low levels of Cux2 staining the gcl neurons, where there was an overlap with the Cux2-cre fate-mapped cells (Supporting Information Fig. S4). Thus Neurod1, like Cux2, may be active in the germinative matrix of the DG, and staining in the gcl at postnatal stages reflects the activity of neurogenic factors during DG formation.

Another possibility explaining the discrepancy between the high Cux2-expressing cells in the SGZ cells and the restriction of the Cux2-ires-Cre fate-mapped cells to the gcl is that the levels of Cux2 in NPs are highly dynamic and rapidly downregulated upon differentiation. Thereafter a persistent low Cux2 level will be maintained in maturing granule cells. This is consistent with the endogenous expression pattern of Cux2 in the neonatal DG, which is highest in Type 1 and Type 2 SGZ progenitors and lowest in DCX$^+$/Calretinin$^+$ nascent neurons and Calbindin$^+$ differentiated granule cells (Figs. 3 and 4). A dynamic expression phenomenon has been observed for the Notch effector Hes1 in cortical NPs (Kageyama et al., 2009). Interestingly, we previously showed that Cux2 is regulated by Notch signaling during spinal cord neurogenesis (Iulianella et al., 2009). Furthermore, during cortical development, Cux2 is transiently expressed in SVZ progenitors of the forebrain, and Cux2 expression is maintained in migrating cortical neurons as they mature into upper layer pyramidal neurons (Zimmer et al., 2004; Cubelos et al., 2008a). Fate mapping during cortical development confirms Cux2 activity in both progenitors and accruing neurons of layers II/III (Franco et al., 2012; Guo et al., 2013). It is possible that Cux2 expression in the SGZ progenitors is transient and rapidly down-regulated upon terminal differentiation. This scenario would explain why the Cux2-ires-Cre fate-mapped cells only show high levels of reporter gene activity in granule cell neurons, reflecting the burst of Cux2 activation in their progenitors and the subsequent down-regulation of Cux2 in granule cells. A third possibility is that the Cux2-ires-Cre line used in this study does not accurately reflect the endogenous expression pattern of Cux2. However, we did observe Cux2 co-staining in Tomato$^+$ fate-mapped cells in the DG (Supporting Information Fig. S4), suggesting the driver accurately reflect endogenous Cux2 locus activity. Together with our expression analysis, our findings are most consistent with the view that Cux2 activity germinal matrix of the developing DG and the postnatal SGZ leads to the progressive labeling of gcl neurons along an outer-to-in maturation gradient.

While most of the highly expressing Cux2 cells in the SGZ were neuroblasts and nascent neurons, a significant number of them were also Type 1 Nestin$^+$/Sox2$^+$ and Type 2 Sox2$^+$/Nestin$^-$ progenitors (Fig. 7B). Interestingly, short-term EdU pulsing experiments and Ki67 staining revealed that Cux2 was expressed in a subset of non-dividing Type1 and 2 progenitors. Furthermore, Cux2 protein was distributed across most types of NPs, consistent with the transition of Type 1 cells to post-mitotic neurons (Figs. 3, 4 and 7B). We did not see much co-localization with Tbr2, but this likely reflects the low

numbers of Tbr2^{+} cells in the SGZ. We suggest that Cux2 expression defines an activated NP undergoing terminal neuronal differentiation to granule cells in the DG. One view is that this represents a novel neuronally restricted (i.e., non-self-renewing) SGZ progenitor type. This intriguing observation may shed light as to whether the postnatal hippocampus contains multipotent self-renewing progenitors vs. lineage-restricted non-self-renewing progenitors or some combination thereof (Bonaguidi et al., 2011; Clarke and van der Kooy, 2011; Encinas et al., 2011; Kempermann, 2011). There is evidence that the hippocampal progenitors contain separate glial and neuronal lineages with limited self-renewal capabilities (Bull and Bartlett, 2005; Clarke and van der Kooy, 2011; Encinas et al., 2011). On the other hand, in vivo clonal analyses of Type 1 cells suggest that they are indeed multipotent and are capable of self-renewal (Suh et al., 2007; Bonaguidi et al., 2011). A possible explanation is that the SGZ may be populated with progenitors from different embryonic sources. Clarke and van der Kooy (2011) argued that the fetal ventricular zone of the presumptive hippocampal-forming region is a source of unipotent progenitors that take up residence in the SGZ. We noted Cux2 expression in the SVZ of the presumptive DG forming region of the forebrain from E14.5 onwards. While co-expression was observed with Prox1^{+} nascent DG neurons, most of the Cux2 expression domain was within the SVZ of the dentate forming region, indicating it is a marker for presumptive SGZ progenitors. Our fate-mapping analysis indicates that Cux2-expressing SVZ progenitors in the dentate primordia directly differentiate into Calbindin^{+} granule cells in the DG and have limited or no capacity for self-renewal. There are several observations in the current study consistent with the idea. First, although Cux2 was expressed in most SGZ progenitors, including Nestin[+]/Sox2^{+} Type 1 cells, Cux2-cre; R26r-tdTomato fate mapping showed a lack of labeling in the SGZ, where NPs self-renew. Secondly, long-term EdU pulse labeling studies revealed that the loss of Cux2 was not accompanied by any changes of the quiescent self-renewing Sox2^{+} progenitor pool. We also observed no co-staining of Cux2 with Ki67, a marker for proliferating progenitors, nor with EdU after a short (6 h) pulse, which labeled Nestin[+] and Sox2^{+} SGZ cells. Lastly, we showed a progressive decline in Cux2^{+} cells in the SGZ from perinatal to adult stages, suggesting that its expression identifies a NP that supplies nascent neurons in the maturing DG at peak neurogenic stages within the first few weeks after birth.

Our findings thus support the notion that the SGZ has a mixed population of progenitors originating from embryonic germinal regions and possessing intrinsic differences in their ability to self-renew. In particular, we argue that Cux2 may act in hippocampal progenitors to restrict their self-renewing abilities and promote granule cell differentiation, similar to its role in promoting neurogenesis in the olfactory epithelium (Wittmann et al., 2014). In support of this, our fate-mapping studies show that Cux2^{+} progenitors generate most Calbindin[+] granule cell neurons in the DG, but not any SGZ progenitors. Moreover, Cux2 activity in the developing DG occurred quite early in the mouse fetus (E14.5) at stages corresponding to the formation of the dentate germinal matrices and migration of granule cell precursors from the germinal wall of the forebrain SVZ (Fig. 7A). In this way Cux2 activity selectively labeled the forming DG in an outside-in manner, as has been described in birth dating studies by Altman and coworkers (Altman and Das, 1965; Altman and Bayer, 1990a,b). This is similar to the proposed role for Cux2 in cell fate restriction in the developing cortex (Franco et al., 2012; Guo et al., 2013). Using a tamoxifen-inducible Cux2-Cre driver, Franco et al. claimed that Cux2 activity defined a class of cortical progenitors fated to give rise to upper layer pyramidal neurons. This has stirred debate in the field and led to another study using Cux2-Cre fate mapping to argue that there is no inherent bias as to the fate of Cux2-expressing cortical progenitors (Guo et al., 2013). However, both studies demonstrate that Cux2 acts within NPs to promote layer-specific differentiation of cortical pyramidal neurons. Here we suggest a similar role for Cux2 reflecting the birth of granule cells in the developing DG along the outer-to-inner formation front.

Despite the expression and fate mapping data suggesting a role for Cux2 in hippocampal neurogenesis, our Cux2 loss-of-function studies did not overtly affect the DG morphogenesis or the formation of Prox1^{+} nascent gcl neurons. The Cux2[neo/neo] allele used in this study is a gene trap mutation that was previously shown to greatly attenuate Cux2 levels in the brain and shows variable penetrance and expressivity in embryonic neurogenic phenotypes (Iulianella et al., 2008; Wittmann et al., 2014). However, in the hippocampus, the Cux2[neo/neo] mutation abolished all Cux2 immunoreactivity, demonstrating the loss of function is complete (Supporting Information Fig. S1). Thus another possibility is that Cux2 acts redundantly with Cux1, which is the other Cux homolog in the mammalian genome. Indeed, previous work demonstrated that Cux1 and Cux2 act together to promote layer specification in the cortex (Cubelos et al., 2008b). Our unpublished observations indicate that Cux1 is also expressed in the SGZ of neonatal and adult DG, supporting a functional redundancy between the two Cux factors.

In conclusion, we provide evidence that Cux2 is a discriminatory marker for non-self-renewing progenitors in the perinatal SGZ of the hippocampus. Our work also sheds light on the molecular patterning of the archicortex. In both the neo- and archicortices, Cux2 appears to play a role in the stratified accretion of newborn neurons. This surprising finding speaks to the deep conservation of genetic programs linking the histogenesis of the ancient parts of the brain with the more recently evolved ones.

REFERENCES

Abercrombie M. 1946. Estimation of nuclear population from microtome sections. Anat Rec 94:239–47.

Altman J. 1969. Autoradiographic and histological studies of postnatal neurogenesis. III. Dating the time of production and onset of differentiation of cerebellar microneurons in rats. J Comp Neurol 136:269–293.

Altman J, Das GD. 1965. Autoradiographic and histological evidence of postnatal hippocampal neurogenesis in rats. J Comp Neurol 124:319–335.

Altman J, Das GD. 1966. Autoradiographic and histological studies of postnatal neurogenesis. I. A longitudinal investigation of the kinetics, migration and transformation of cells incorporating tritiated thymidine in neonate rats, with special reference to postnatal neurogenesis in some brain regions. J Comp Neurol 126:337–389.

Altman J, Bayer SA. 1990a. Migration and distribution of two populations of hippocampal granule cell precursors during the perinatal and postnatal periods. J Comp Neurol 301:365–381.

Altman J, Bayer SA. 1990b. Mosaic organization of the hippocampal neuroepithelium and the multiple germinal sources of dentate granule cells. J Comp Neurol 301:325–342.

Aprea J, Nonaka-Kinoshita M, Calegari F. Generation and characterization of Neurod1-CreER mouse lines for the study of embryonic and adult neurogenesis. Genesis (in press). DOI: 10.1002/dvg.22797.

Bonaguidi MA, Wheeler MA, Shapiro JS, Stadel RP, Sun GJ, Ming GL, Song H. 2011. In vivo clonal analysis reveals self-renewing and multipotent adult neural stem cell characteristics. Cell 145:1142–1155.

Brandt MD, Jessberger S, Steiner B, Kronenberg G, Reuter K, Bick-Sander A, von der Behrens W, Kempermann G. 2003. Transient calretinin expression defines early postmitotic step of neuronal differentiation in adult hippocampal neurogenesis of mice. Mol Cell Neurosci 24:603–613.

Bull ND, Bartlett PF. 2005. The adult mouse hippocampal progenitor is neurogenic but not a stem cell. J Neurosci 25:10815–10821.

Burns TC, Verfaillie CM, Low WC. 2009. Stem cells for ischemic brain injury: A critical review. J Comp Neurol 515:125–144.

Clarke L, van der Kooy D. 2011. The adult mouse dentate gyrus contains populations of committed progenitor cells that are distinct from subependymal zone neural stem cells. Stem Cells 29:1448–1458.

Cubelos B, Sebastian-Serrano A, Kim S, Moreno-Ortiz C, Redondo JM, Walsh CA, Nieto M. 2008a. Cux-2 controls the proliferation of neuronal intermediate precursors of the cortical subventricular zone. Cereb Cortex 18:1758–1770.

Cubelos B, Sebastian-Serrano A, Kim S, Redondo JM, Walsh C, Nieto M. 2008b. Cux-1 and Cux-2 control the development of Reelin expressing cortical interneurons. Dev Neurobiol 68:917–25.

D'Amour KA, Gage FH. 2003. Genetic and functional differences between multipotent neural and pluripotent embryonic stem cells. Proc Natl Acad Sci USA 100 (Suppl 1): 11866–11872.

Encinas JM, Michurina TV, Peunova N, Park JH, Tordo J, Peterson DA, Fishell G, Koulakov A, Enikolopov G. 2011. Division-coupled astrocytic differentiation and age-related depletion of neural stem cells in the adult hippocampus. Cell Stem Cell 8:566–579.

Ferri AL, Cavallaro M, Braida D, Di Cristofano A, Canta A, Vezzani A, Ottolenghi S, Pandolfi PP, Sala M, DeBiasi S, Nicolis SK. 2004. Sox2 deficiency causes neurodegeneration and impaired neurogenesis in the adult mouse brain. Development 131:3805–3819.

Franco SJ, Gil-Sanz C, Martinez-Garay I, Espinosa A, Harkins-Perry SR, Ramos C, Muller U. 2012. Fate-restricted neural progenitors in the mammalian cerebral cortex. Science 337:746–749.

Guo C, Eckler MJ, McKenna WL, McKinsey GL, Rubenstein JLR, Chen B. 2013. Fezf2 expression identifies a multipotent progenitor for neocortical projection neurons, astrocytes, and oligodendrocytes. Neuron 80:1167–1174.

Hodge RD, Kowalczyk TD, Wolf SA, Encinas JM, Rippey C, Enikolopov G, Kempermann G, Hevner RF. 2008. Intermediate progenitors in adult hippocampal neurogenesis: Tbr2 expression and coordinate regulation of neuronal output. J Neurosci 28:3707–3717.

Iulianella A, Vanden Heuvel G, Trainor P. 2003. Dynamic expression of murine Cux2 in craniofacial, limb, urogenital and neuronal primordia. Gene Expr Patterns 3:571–577.

Iulianella A, Sharma M, Durnin M, Vanden Heuvel GB, Trainor PA. 2008. Cux2 (Cutl2) integrates neural progenitor development with cell-cycle progression during spinal cord neurogenesis. Development 135:729–741.

Iulianella A, Sharma M, Vanden Heuvel GB, Trainor PA. 2009. Cux2 functions downstream of Notch signaling to regulate dorsal interneuron formation in the spinal cord. Development 136:2329–2334.

Kageyama R, Ohtsuka T, Shimojo H, Imayoshi I. 2009. Dynamic regulation of Notch signaling in neural progenitor cells. Curr Opin Cell Biol 21:733–740.

Kempermann G. 2006. Adult Neurogenesis: Stem Cells and Neuronal Development in the Adult Brain. New York: Oxford University Press.

Kempermann G. 2011. The pessimist's and optimist's views of adult neurogenesis. Cell 145:1009–1011.

Kempermann G, Jessberger S, Steiner B, Kronenberg G. 2004. Milestones of neuronal development in the adult hippocampus. Trends Neurosci 27:447–452.

Kernie SG, Parent JM. 2010. Forebrain neurogenesis after focal ischemic and traumatic brain injury. Neurobiol Dis 37:267–274.

Kriegstein A, Alvarez-Buylla A. 2009. The glial nature of embryonic and adult neural stem cells. Annu Rev Neurosci 32:149–184.

Kuhn HG, Dickinson-Anson H, Gage FH. 1996. Neurogenesis in the dentate gyrus of the adult rat: Age-related decrease of neuronal progenitor proliferation. J Neurosci 16:2027–2033.

Lavado A, Oliver G. 2007. Prox1 expression patterns in the developing and adult murine brain. Dev Dyn 236:518–524.

Lazarov O, Mattson MP, Peterson DA, Pimplikar SW, van Praag H. 2010. When neurogenesis encounters aging and disease. Trends Neurosci 33:569–579.

Li G, Pleasure SJ. 2005. Morphogenesis of the dentate gyrus: What we are learning from mouse mutants. Dev Neurosci 27:93–99.

Lichtenwalner RJ, Parent JM. 2006. Adult neurogenesis and the ischemic forebrain. J Cereb Blood Flow Metab 26:1–20.

Liu J, Suzuki T, Seki T, Namba T, Tanimura A, Arai H. 2006. Effects of repeated phencyclidine administration on adult hippocampal neurogenesis in the rat. Synapse 60:56–68.

Liu Y, Namba T, Liu J, Suzuki R, Shioda S, Seki T. 2010. Glial fibrillary acidic protein-expressing neural progenitors give rise to immature neurons via early intermediate progenitors expressing both glial fibrillary acidic protein and neuronal markers in the adult hippocampus. Neuroscience 166:241–251.

Lopez-Toledano MA, Ali Faghihi M, Patel NS, Wahlestedt C. 2010. Adult neurogenesis: A potential tool for early diagnosis in Alzheimer's disease? J Alzheimers Dis 20:395–408.

Madisen L, Zwingman TA, Sunkin SM, Oh SW, Zariwala HA, Gu H, Ng LL, Palmiter RD, Hawrylycz MJ, Jones AR, Lein ES, Zeng H. 2010. A robust and high-throughput Cre reporting and characterization system for the whole mouse brain. Nat Neurosci 13:133–140.

Ming GL, Song H. 2011. Adult neurogenesis in the mammalian brain: Significant answers and significant questions. Neuron 70:687–702.

Mouton PR. 2002. Principles and Practices of Unbiased Stereology: An Introduction for Bioscientists. Baltimore: Johns Hopkins University Press.

Nakatomi H, Kuriu T, Okabe S, Yamamoto S, Hatano O, Kawahara N, Tamura A, Kirino T, Nakafuku M. 2002. Regeneration of hippocampal pyramidal neurons after ischemic brain injury by recruitment of endogenous neural progenitors. Cell 110:429–441.

Nieto M, Monuki ES, Tang H, Imitola J, Haubst N, Khoury SJ, Cunningham J, Gotz M, Walsh CA. 2004. Expression of Cux-1 and Cux-2 in the subventricular zone and upper layers II-IV of the cerebral cortex. J Comp Neurol 479:168–180.

Palmer TD, Willhoite AR, Gage FH. 2000. Vascular niche for adult hippocampal neurogenesis. J Comp Neurol 425:479–494.

Rickmann M, Amaral DG, Cowan WM. 1987. Organization of radial glial cells during the development of the rat dentate gyrus. J Comp Neurol 264:449–479.

Seki T, Arai Y. 1999. Temporal and spacial relationships between PSA-NCAM-expressing, newly generated granule cells, and radial glia-like cells in the adult dentate gyrus. J Comp Neurol 410:503–513.

Seri B, Garcia-Verdugo JM, McEwen BS, Alvarez-Buylla A. 2001. Astrocytes give rise to new neurons in the adult mammalian hippocampus. J Neurosci 21:7153–7160.

Seri B, Garcia-Verdugo JM, Collado-Morente L, McEwen BS, Alvarez-Buylla A. 2004. Cell types, lineage, and architecture of the germinal zone in the adult dentate gyrus. J Comp Neurol 478: 359–378.

Sohur US, Emsley JG, Mitchell BD, Macklis JD. 2006. Adult neurogenesis and cellular brain repair with neural progenitors, precursors and stem cells. Philos Trans R Soc Lond B Biol Sci 361:1477–1497.

Steiner B, Zurborg S, Horster H, Fabel K, Kempermann G. 2008. Differential 24 h responsiveness of Prox1-expressing precursor cells in adult hippocampal neurogenesis to physical activity, environmental enrichment, and kainic acid-induced seizures. Neuroscience 154:521–529.

Suh H, Consiglio A, Ray J, Sawai T, D'Amour KA, Gage FH. 2007. In vivo fate analysis reveals the multipotent and self-renewal capacities of Sox2+ neural stem cells in the adult hippocampus. Cell Stem Cell 1:515–528.

Wang C, Zhang M, Sun C, Cai Y, You Y, Huang L, Liu F. 2011. Sustained increase in adult neurogenesis in the rat hippocampal dentate gyrus after transient brain ischemia. Neurosci Lett 488:70–75.

Wittmann W, Iulianella A, Gunhaga L. 2014. Cux2 acts as a critical regulator for neurogenesis in the olfactory epithelium of vertebrates. Dev Biol 388:35–47.

Yu Y, He J, Zhang Y, Luo H, Zhu S, Yang Y, Zhao T, Wu J, Huang Y, Kong J, Tan Q, Li XM. 2009. Increased hippocampal neurogenesis in the progressive stage of Alzheimer's disease phenotype in an APP/PS1 double transgenic mouse model. Hippocampus 19:1247–1253.

Zhang C, McNeil E, Dressler L, Siman R. 2007. Long-lasting impairment in hippocampal neurogenesis associated with amyloid deposition in a knock-in mouse model of familial Alzheimer's disease. Exp Neurol 204:77–87.

Zimmer C, Tiveron MC, Bodmer R, Cremer H. 2004. Dynamics of Cux2 expression suggests that an early pool of SVZ precursors is fated to become upper cortical layer neurons. Cereb Cortex 14: 1408–1420.